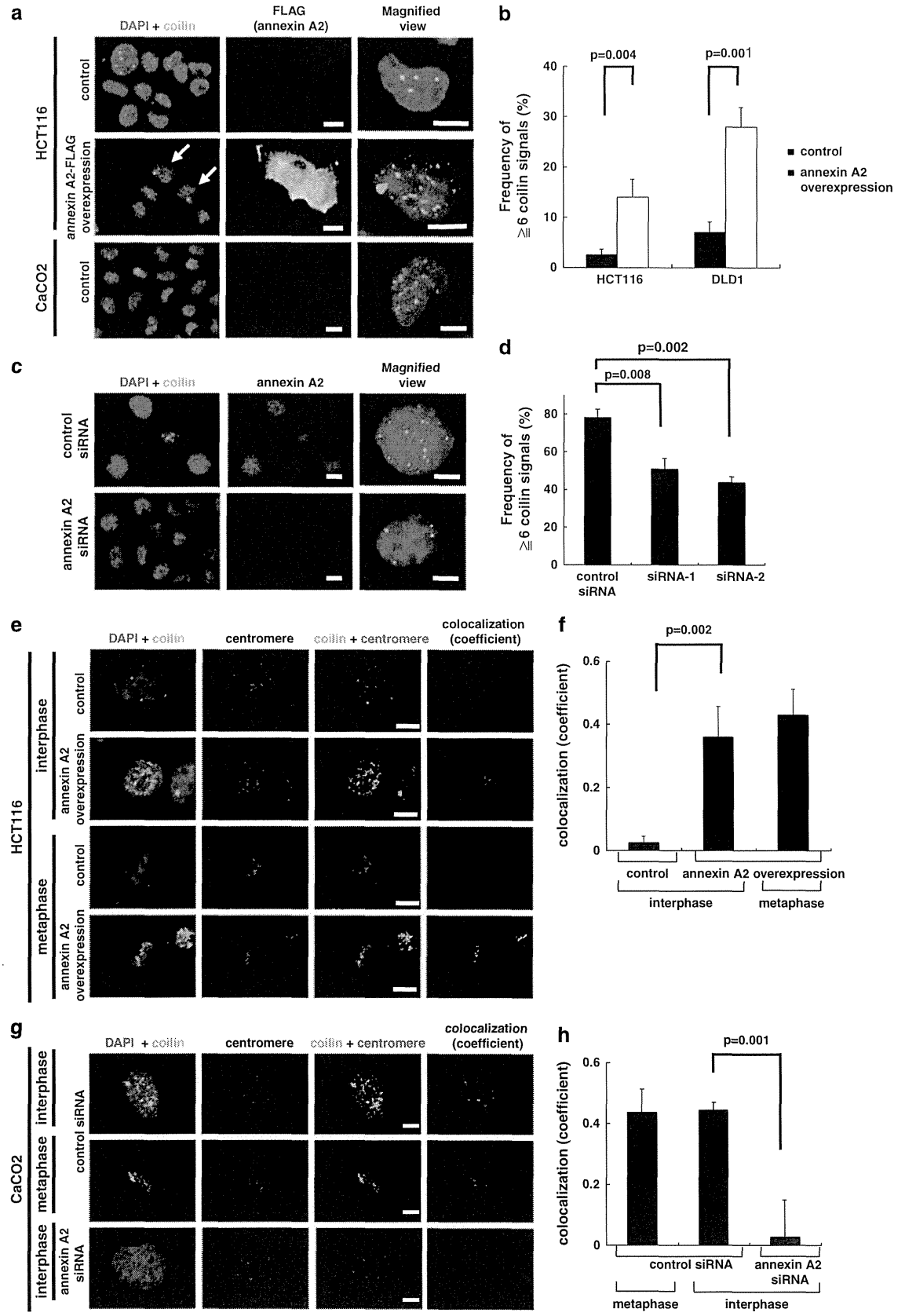

Figure 5. For caption please see next page.

We then tested whether the disassembled CB localize to the centromere. Immunostaining of annexin A2-FLAG-overexpressed HCT116 cells with anti-coilin and anti-centromere antibodies showed that coilin partially colocalizes with the centromere in annexin-FLAG-overexpressed cells either in interphase or metaphase (Figure 5e, Supplementary Figure S5). We quantified the degree of colocalization between coilin and centromeres both in control and transfected cells using confocal microscopy and colocalization software. Coilin showed higher values of the Pearson's correlation coefficient with centromeres (0.36 ± 0.10) in annexin A2-overexpressed HCT116 cells, as well as CaCO2 cells as compared with HCT116 cells both in interphase and metaphase (Figures 5f and h). Colocalization of coilin with centromeres in annexin A2-overexpressed MIN cells and control CIN cells was also observed in several stages of mitosis during prophase and metaphase, whereas coilin localized uniformly, but not in the chromatin region, in the cells during anaphase/telophase (Supplementary Figure S5). Conversely, when annexin A2 was knocked down in CaCO2 cells, scattered coilin returned to the several large stained foci as seen in MIN cells (Figure 5g), and the high Pearson's correlation coefficient between coilin and centromeres decreased (Figure 5h). This colocalization pattern in annexin A2-overexpressed MIN cells and control CIN cells resembles the coilin distribution at the centromere upon herpes simplex virus type 1 infection,[31] and is suggestive of aberrant centromere function induced by annexin A2 overexpression.

Ectopic expression of annexin A2 in MIN cells significantly reduces expression of CENPs, which is due to aberrant localization of coilin

To test whether annexin A2 overexpression interferes with centromere function, several CENPs were examined by immunostaining with specific antibodies. CENP-A and C are the well-conserved core CENPs responsible for proper chromosome segregation, and their reduced expression has been shown to cause chromosome missegregation *in vitro* and *in vivo*.[33–35] Thus, we examined the levels of CENP-A and C in annexin A2-FLAG-overexpressed cells. Intriguingly, dot signals for CENP-A and -C were significantly reduced in the annexin A2-overexpressed HCT116 cells both in interphase and mitosis, and the intensity of CENP-A and -C staining in annexin A2-overexpressed HCT116 cells was markedly lower than in control cells (Figures 6a–c; Supplementary Figures S6a–c).

To determine if scattered coilin is required for reduced expression of CENP-A and -C by annexin A2 overexpression, coilin was depleted by siRNA in annexin A2-overexpressed HCT116 cells. As expected, dot signals and their intensities for CENP-A and -C were restored in these cells (Figures 6a and b; Supplementary Figures S6a and c). These results suggest that enhanced annexin A2 localization in the nucleus interferes with proper centromeric protein assembly by recruiting coilin to the centromere and/or mitotic chromosome.

To further investigate if this reduced staining of CENP-A and -C is because of reduced levels of centromeric proteins or displacement of these proteins from the centromere, we performed western blotting of nuclear cell extracts obtained from annexin A2-FLAG-overexpressed MIN cells. Both CENP-A and -C expression were decreased in the annexin A2-overexpressed cells (Figures 6d and e). We also tested if the reduced expression level of CENPs in the cells overexpressing annexin A2 can be restored by knockdown of coilin. As anticipated, CENP-C and CENP-A levels were partially restored in cells overexpressing annexin A2 in a coilin knockdown background (Figures 6d and e).

To examine whether the decrease of CENP-A and -C occurred at the mRNA level, a set of primers that specifically amplifies CENP-A and -C were designed, and real-time quantitative RT–PCR was carried out using total RNA extracted from annexin A2-overexpressed and control cells. The CENP-A and -C mRNA levels did not differ between the annexin A2-overexpressed cells and control cells (Supplementary Figures S6d and e). These results suggest that nuclear annexin A2 accumulation causes CIN by coilin-mediated reduced CENP expression.

Next, to investigate whether the reduced expression of CENP-A and CENP-C was because of their degradation, we examined the expression level of CENPs in the cells overexpressing annexin A2 with and without the proteasomal inhibitor MG132. Strikingly, CENP-C and CENP-A levels were restored in cells overexpressing annexin A2 with MG132 treatment (Figures 6f and g). These results suggest that coilin might recruit an E3 ubiquitin ligase to the centromeres to induce proteasomal degradation of CENPs.

Annexin A2-knockdown in CIN cells increases the expression of CENPs and the endogenous expression levels of CENPs in CIN cells are greatly reduced compared with MIN cell lines

To test how the suppression of annexin A2 exerts influence on CENPs, CIN cells were treated with annexin A2 siRNAs, and centromere proteins CENP-A and CENP-C were immunostained. Control CaCO2 cells showed faint signals in the nucleus; however, siRNA-treated CaCO2 cells showed clear, strong signals both in interphase and mitosis, and the intensity of CENP-A and -C staining in siRNA-treated cells was markedly higher than in control siRNA-treated cells (Figures 7a–c; Supplementary Figures S7a and b).

To examine the expression levels of CENPs, western blotting of CENP-A and -C was performed using nuclear extracts of annexin

Figure 5. Annexin A2 overexpression in MIN cells induces disassembly and colocalization of coilin with centromeres, whereas suppression of annexin A2 in CIN cells converges scattered coilin. (**a**) Localization of coilin in annexin A2-overexpressed MIN cells and control CIN cells. Annexin A2-FLAG was transfected into HCT116 cells, and the localization of coilin was examined with anti-coilin antibody after 72 h. Scattered coilin staining was observed in the nuclei of annexin A2-FLAG-overexpressed HCT116 cells (arrow), but not in control cells. Scattered coilin staining was also observed in control CaCO2 cells. (**b**) Frequency of cells with coilin scattering (containing $\geqslant 6$ coilin signals) in annexin A2-overexpressed MIN cells. Coilin signals were counted in at least 300 cells. (**c**) Localization of coilin in annexin A2-knockdown CIN cells. Annexin A2 siRNA was transfected into CaCO2 cells, and the localization of coilin was examined with anti-coilin antibody after 96 h. Scattered coilin staining was converged and several large foci were observed in the nuclei of annexin A2 siRNA-treated cells (lower panel). (**d**) Frequency of cells with coilin scattering (containing $\geqslant 6$ coilin signals) in annexin A2-knockdown CIN cells. Coilin signals in the control and annexin A2 siRNA-treated CaCO2 cells were counted in at least 300 cells. (**e**) Localization of coilin and centromeres in annexin A2-overexpressed HCT116 cells in interphase and metaphase. Coilin and centromeres were immunostained with anti-coilin and anti-centromere antibodies in control and annexin A2-overexpressed HCT116 cells. Overexpression of annexin A2 induced partial localization of coilin to the centromeres both in interphase and metaphase. (**f**) Frequency of colocalization between coilin and centromeres in control and annexin A2-overexpressed HCT cells in interphase and metaphase. Colocalization of coilin and centromeres was examined using confocal microscopy, and Pearson's correlation coefficient was calculated. Data are presented as the means $\pm$ s.d. At least 50 cells were quantified. (**g**) Localization of coilin and centromeres in annexin A2-knockdown CaCO2 cells in interphase and metaphase. Control and annexin A2 siRNA was transfected into CaCO2 cells, and the localization of coilin and centromeres was examined with anti-coilin and anti-centromere antibodies after 96 h. Scattered coilin staining was converged and several large foci were observed in the nuclei of annexin A2 siRNA-treated cells. (**h**) Frequency of colocalization between coilin and centromeres in annexin A2-knockdown CaCO2 cells. Colocalization (correlation coefficient) was quantified using confocal microscopy and colocalization software. At least 50 cells were quantified. Bar, 10 μm.

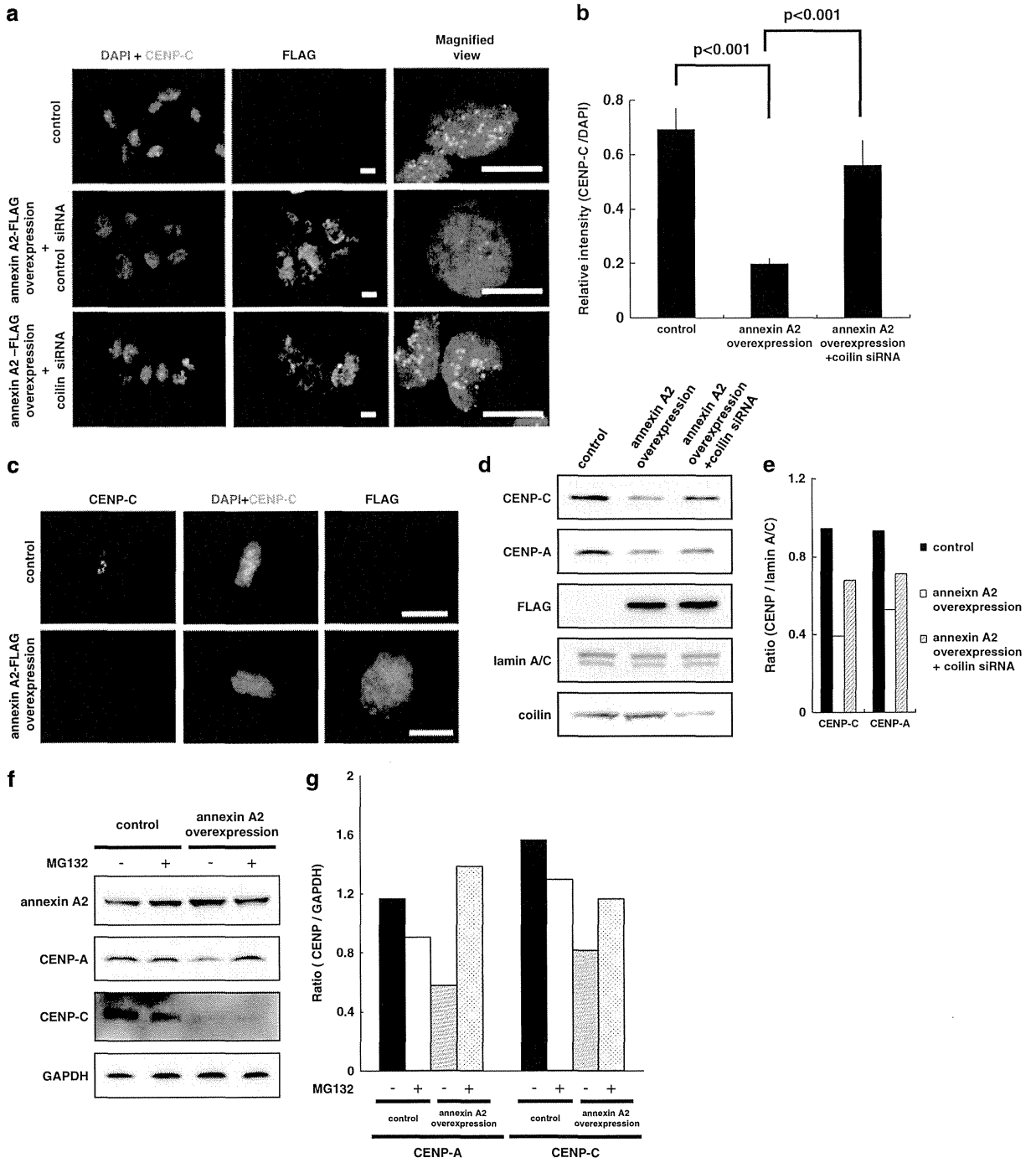

Figure 6. Expression of centromere proteins is reduced by annexin A2 overexpression but restored by repression of coilin. (**a**) Immunostaining of centromere protein C (CENP-C) in annexin A2-overexpressed MIN cells. Annexin A2-FLAG was transfected with or without coilin siRNA into HCT116 cells, and CENP-C and annexin A2 were immunostained with CENP-C and FLAG antibodies after 72 h in control (upper panels), annexin A2-overexpressed (middle panels), and annexin A2-FLAG and coilin siRNA co-transfected cells (lower panels). Annexin A2-overexpressed cells showed reduced CENP-C signals, whereas coilin siRNA co-transfected cells restored the attenuated CENP-C signals. Magnified views are shown in the panels on the right. (**b**) Relative intensities between CENP-C and DAPI in control, annexin A2-overexpressed, and annexin A2-FLAG and coilin siRNA co-transfected HCT116 cells. Intensities of CENP-C and DAPI staining were analyzed in at least 150 cells using AxioVision software, and relative intensities of CENP-C as compared with DAPI were calculated. (**c**) Immunostaining of CENP-C in annexin A2-overexpressed mitotic HCT116 cells. Bar, 10 μm. (**d**) Western blot analysis of CENP proteins in control, annexin A2-overexpressed, and annexin A2-FLAG and coilin siRNA co-transfected HCT116 cells. The expressions of CENP-A and CENP-C in nuclear extracts were examined with anti-CENP-A and CENP-C antibodies 72 h after transfection. Equal loading of protein was confirmed using anti-lamin A/C antibody. (**e**) Ratio of CENP and lamin A/C expression in control, annexin A2-overexpressed, and annexin A2-FLAG and coilin siRNA co-transfected cells. The intensities of the bands were analyzed using Scion Image software. (**f**) Western blot analysis of CENP proteins in annexin A2-overexpressed HCT116 cells with or without proteasomal inhibitor MG132 treatment. The expressions of CENP-A and CENP-C in nuclear extracts with or without 2-h MG132 treatment were examined. (**g**) Ratio of CENP and GAPDH expression in annexin A2-overexpressed HCT116 cells with or without MG132 treatment.

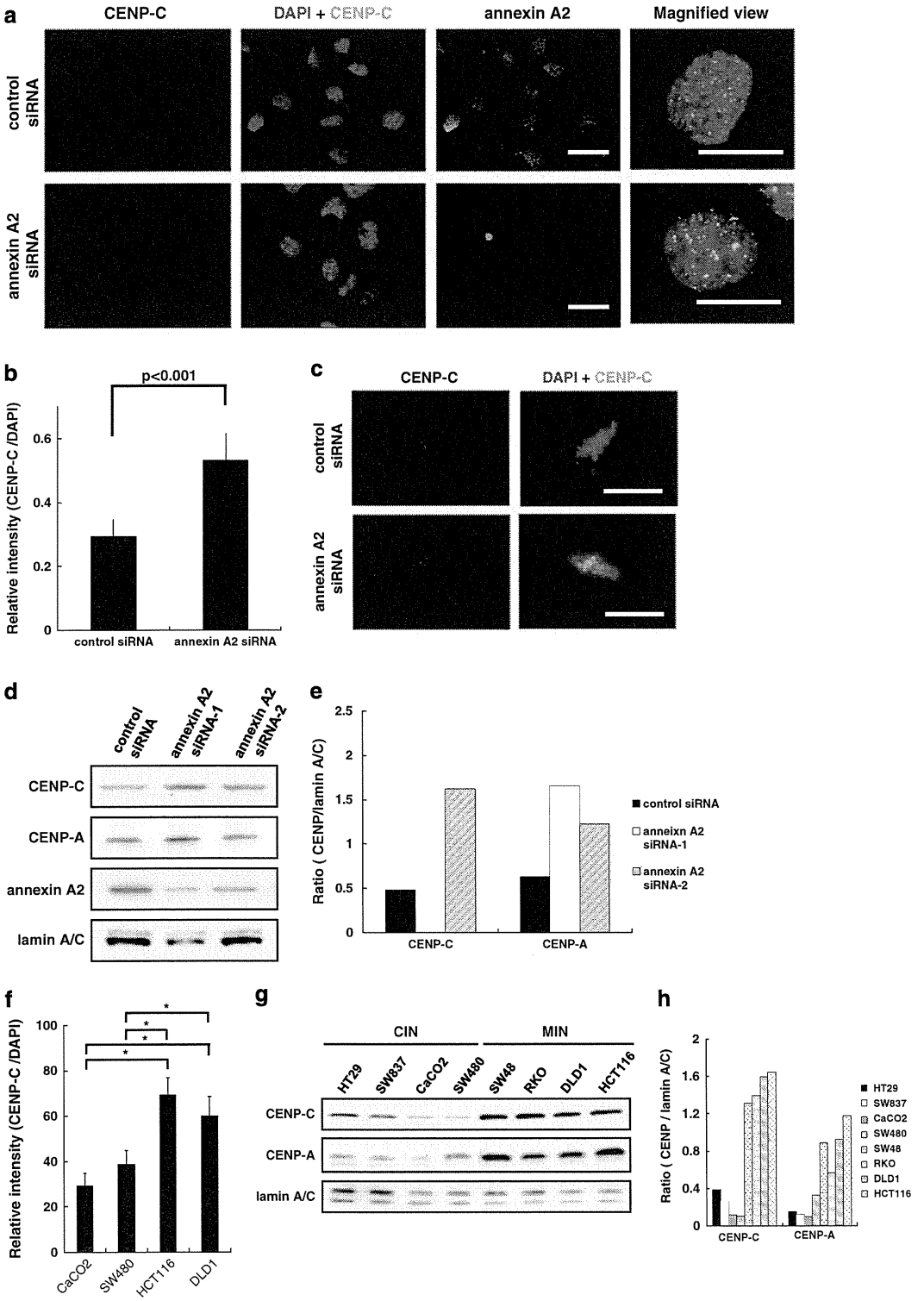

Figure 7. Suppression of annexin A2 in CIN cells increases expression of centromere proteins and the endogenous expression levels of centromere proteins in CIN cells are greatly reduced compared with MIN cell lines. (**a**) Immunostaining of CENP-C in annexin A2-knockdown CIN cells. Control and annexin A2 siRNA were transfected into CaCO2 cells, and CENP-C and annexin A2 were immunostained with CENP-C and annexin A2 antibodies after 72 h. (**b**) Relative intensities between CENP-C and DAPI in control and annexin A2 siRNA-treated CaCO2 cells. Intensities of CENP-C and DAPI staining were analyzed in at least 150 cells using AxioVision software, and relative intensities of CENP-C as compared with DAPI were calculated. (**c**) Immunostaining of CENP-C in annexin A2-knockdown mitotic CaCO2 cells. Bar, 10 μm. (**d**) Western blot analysis of CENP proteins in annexin A2-knockdown CaCO2 cells. Expressions of CENP-A and CENP-C in the nuclear extracts were examined with anti-CENP-A and CENP-C antibodies 72 h after transfection. Equal loading of protein was confirmed using anti-lamin A/C antibody. (**e**) Ratio of CENP and lamin A/C expression in annexin A2-knockdown CaCO2 cells. (**f**) Relative intensity between CENP-C and DAPI in CIN and MIN cells. At least 100 cells were quantified. Bar, 10 μm. (**g**) Western blot analysis of CENP proteins in CIN and MIN cells. (**h**) Ratio of CENP and lamin A/C expression in CIN and MIN cells. *$P \leqslant 0.05$ by Wilcoxon-Mann-Whitney test.

A2 siRNA-treated CaCO2 cells. As expected, the expressions of both CENP-A and -C were increased in the annexin A2-knockdown cells (Figures 7d and e). The CENP-A and -C mRNA levels did not differ between the annexin A2-knockdown cells and control cells (Supplementary Figures S7c and d).

Finally, we examined the endogenous expression levels of CENPs in CIN and MIN cell lines with immunostaining and western blotting. Dot signals for CENP-A and -C and their intensity in immunostaining images were significantly lower in CIN cells than MIN cells (Figure 7f), and CENP-A and -C expression levels in western blots were greatly reduced in CIN cells compared with MIN cells (Figures 7g and h). These observations further support the hypothesis that nuclear annexin A2 accumulation is necessary and sufficient for aberrant expression of core CENPs, which would be the fundamental mechanism of CIN.

DISCUSSION

In this study, we found that overexpression of annexin A2 in MIN cells leads to a marked induction of aneuploidy and CIN, whereas repression of annexin A2 expression in CIN cells reduces the characteristic heterogeneity of the chromosome number associated with CIN. Enhanced nuclear annexin A2 levels in MIN cells leads to the scattering of coilin with partial localization to the centromeres in interphase and mitosis. Strikingly, nuclear accumulation of annexin A2 reduced CENP expression. Conversely, knockdown of annexin A2 in CIN cells produced exactly the opposite effect on localization of coilin and CENP expression. The endogenous expression levels of CENPs in CIN cells were also greatly reduced compared with MIN cell lines. Furthermore, the reduction of centromere signals in annexin A2-overexpressed MIN cells was restored by the depletion of coilin. Our results strongly suggest that nuclear localization of annexin A2 impedes centromere function due to aberrant localization of coilin to the centromeres, thereby promoting development of CIN.

CIN has been recognized to occur by chromosome segregation errors, and kinetochore-microtubule attachment error (for example, merotelic attachment) is a common cause of CIN.[17] Perturbation of centromere/kinetochore proteins reduces segregation fidelity due to elevation of kinetochore-microtubule malattachment, and a number of these proteins have been reported to elevate the frequency of merotely and lagging chromosomes in anaphase, such as Kif2b, MCAK, CENP-E, CENP-F, the Ndc80 complex, Aurora B and Sgo2.[36] Some of these proteins have been shown to be mutated or underexpresssed in cancer, whereas others are overexpressed, which is a potential cause of increasing kMT stability. We have also reported that the core kinetochore proteins CENP-A and CENP-H are overexpressed in colorectal cancers, and that ectopic expression of these proteins induces aneuploidy.[19,20,37] Thus, appropriate quantities of kinetochore proteins might be crucial for proper chromosome segregation.

Annexins localize primarily in the cytoplasm and have been implicated in a wide variety of general cellular processes, including mitogenic signal transduction, apoptosis and cellular transformation.[22] Although none of the annexins contain nuclear localization signals, the presence of annexins A1, A2, A4, A5 and A11 in the nucleus has been documented.[22] Moreover, annexin A2 has been reported to contain an NES sequence, and the nuclear export inhibitor leptomycin B causes annexin A2 to accumulate in nuclei.[29] Liu *et al.*[38] showed that nuclear annexin A2 is phosphorylated, and that mutation of serines 11 and 25 in the amino terminus prevents nuclear localization. Our observation that endogenous annexin A2 or exogenously expressed annexin A2-GFP localizes in the nucleus of colon cancer cells after leptomycin B treatment confirms the shuttling of annexin A2 between the cytoplasm and nucleus.

How then does excess annexin A2 in the nucleus contribute to CIN? Previous reports showed that nuclear annexin A2 co-purifies with a primer recognition complex and enhances DNA polymerase alpha activity, suggesting a role for annexin A2 in DNA replication.[23,24] Tomas *et al.*[39] showed that annexin 11 has an essential role in the terminal phase of cytokinesis. In this study, we searched for factors that interact with nuclear annexin A2 and identified a major component of CB, coilin. Ectopic expression of annexin A2 in the nucleus induced marked aberrant scattering of coilin and partial localization of coilin to the centromeres in interphase and mitosis. Moreover, the staining intensity of several CENPs was significantly reduced, further supporting the hypothesis that centromeres are damaged upon annexin A2 overexpression.

Previous reports demonstrated that coilin accumulates at the centromere as a result of centromere damage induced by herpes simplex virus type 1 infection, which leads a viral protein, ICP0, a RING finger nuclear protein with E3 ubiquitin ligase activity, to induce proteasomal degradation of CENP-A, -B and -C.[31,40,41] Thus, coilin might recruit some as yet unknown E3 ubiquitin ligases to the centromeres and degrade CENPs. In fact, when coilin was depleted in annexin A2-overexpressed HCT116 cells, the expression of CENP-A and -C was restored in these cells (Figure 6a, Supplementary Figure S5a), indicating that coilin is required for reduced expression of CENPs by annexin A2 overexpression. These results indicate that the presence of coilin at centromeres in annexin A2-overexpressed cells could be the cause of CENPs degradation and not the consequence, unlike what has been previously described for herpes simplex virus type 1-infected cells. The strong interaction between annexin A2 and coilin observed in our experiments suggests that annexin A2 nuclear localization impedes the autointeraction of coilin, localizing coilin to the centromeres and causing centromere damage. The precise mechanism of coilin accumulation at the centromere and the decreased expression of several CENPs awaits further investigation.

CIN has been reported to contribute to cellular resistance to chemotherapeutic drugs.[42,43] We and others recently reported that annexin A2 overexpression is involved in resistance to chemotherapy in pancreatic and breast cancer cell lines;[44,45] thus, annexin A2 overexpression may have a role in the acquisition of chemoresistance and contribute to cancer progression by inducing CIN in cancer cells. If this were the case, annexin A2 is a potential therapeutic target for the prevention of chemoresistance and cancer recurrence.

MATERIALS AND METHODS

Cell culture

All colorectal cancer cell lines were purchased from ATCC (Manassas, VA, USA). Leptomycin B was purchased from Wako (Tokyo, Japan).

Plasmid DNA and antibodies

The annexin A2-FLAG and annexin A2 plasmids were generated by PCR amplification of full-length annexin A2 cDNA and cloning into the p3xFLAG-CMV^{TM}-14 vector plasmid (Sigma-Aldrich, St Louis, MO, USA) and pcDNA 3.1(+) (Invitrogen, Carlsbad, CA, USA), respectively. Antibodies against the following proteins were purchased: mouse anti-annexin A2 (BD Biosciences, Franklin Lakes, NJ, USA), mouse anti-lamin A/C (Santa Cruz Biotechnology, Inc., Santa Cruz, CA, USA), mouse anti-GAPDH (Abcam, Cambridge, UK), mouse anti-FLAG (Sigma-Aldrich), rabbit anti-FLAG (DYKDDDDK) (MBL, Nagoya, Japan), mouse anti-coilin (Abcam), mouse anti-CENP-A (MBL) and rabbit anti-CENP-C (Abcam).

Extraction of nuclear protein

Cells (~1×10^8) were resuspended in 5 ml cold buffer (50 mM phosphate, pH 8.0), 20 mM NaCl, 1 mM DTT, 0.1% NP-40 and protease inhibitor cocktail (Roche Diagnostics, Basel, Switzerland), and were allowed to swell on ice for 15 min. Cells were then homogenized using a Dounce homogenizer or vigorously vortexed twice for 15 s, and then centrifuged for 5 min at

100 × *g*. The pellet was washed twice with the same cold buffer and solubilized in either lysis buffer (7 M urea, 2 M thiourea, 4% (w/v) CHAPS, 30 mM Tris–HCl, protease inhibitor cocktail (Roche Diagnostics)) for 2D-DIGE and western blotting or in 50 mM phosphate buffer (pH 8.0), 150 mM NaCl, 1 mM DTT, 0.1% NP-40 and protease inhibitor cocktail for immunoprecipitation, and centrifuged for 10 min at 20 000 × *g*.

Immunoprecipitation

The nuclear extract was reacted for 1 h at 4 °C with Magnosphere MS300/carboxyl magnetic beads (Cosumo Bio, Tokyo, Japan) precoated with anti-mouse IgG to reduce nonspecific protein binding and then reacted with anti-FLAG antibody for 1 h at 4 °C. After immunoprecipitation, the FLAG beads were washed five times with the same 50 mM phosphate buffer, and bound proteins were eluted with extraction buffer (40 mM Tris–HCl pH 6.8, 1% SDS, 1 mM DTT) for 1 h at 60 °C.

Western blotting, immunostaining, FISH and real-time quantitative PCR

Western blotting, immunostaining, FISH and real-time quantitative PCR were performed as described previously.[19,20] Briefly, nuclear and whole cell extracts were separated by electrophoresis on 10–20% gradient gels (DRC, Tokyo, Japan). Proteins were transferred to polyvinylidene fluoride membranes (Millipore, Bedford, MA, USA) in a tank transfer apparatus (Bio-Rad, Hercules, CA, USA), and the membranes were blocked with 0.5% skimmed milk in phosphate-buffered saline. Anti-annexin A2 antibody diluted 1:1000, anti-lamin A/C antibody diluted 1:250, anti-GAPDH antibody diluted 1:100 000, anti-cleaved caspase 3 antibody (Cell Signaling Technology, Danvers, MA, USA) diluted 1:100, anti-cleaved PARP antibody (Cell Signaling Technology) diluted 1:1000, anti-CENP-A antibody diluted 1:1000, anti-CENP-C antibody diluted 1:200, anti-coilin antibody diluted 1:1000, anti-FLAG antibody diluted 1:1000 were used as primary antibodies. Rabbit anti-mouse IgG HRP (DAKO, Glostrup, Denmark) diluted 1:1000, donkey anti-rabbit IgG HRP (Amersham Pharmacia Biotech, Piscataway, NJ, USA) diluted 1:3000 in blocking buffer were used as secondary antibodies. Antigens on the membrane were detected by enhanced chemiluminescence detection reagents (Amersham Pharmacia Biotech). The intensity of each band was measured by Scion Image software. For immunostaining, anti-CENP-A and -CENP-C antibodies were diluted 1:250 and 1:100, respectively. FISH probes to the pericentromeric regions of chromosomes 7, 8, 10, 12, 15 and 17 were purchased from Vysis (Downers Grove, IL, USA). DNA was stained with 100 ng/ml of DAPI (4′-6-diamidino-2-phenylindole; Sigma-Aldrich). The stained samples were viewed under an Axio Imager Z1 microscope or LSM510 confocal microscope (Carl Zeiss, Jena, Germany) and the images were captured using AxioVision software and LSM510 softwere (Carl Zeiss). The objective lenses were EC Plan-NEO FLUAR 106/0.3 or 406/1.3 and Plan APOCHROMAT 636/1.4. The intensities of annexin A2, CENP-A and CENP-C expression were analyzed using AxioVision software. Pearson's correlation coefficient was calculated using Zen software according to the manufacturer's instructions. The value can range from 0 to 1, with 1 indicating a complete positive correlation and with 0 indicating no correlation. The primer set sequences used in real-time quantitative PCR are listed in Supplementary Table 1.

RNA interference experiments

The siRNA duplexes were purchased from Sigma-Aldrich. The target sequences of siRNA are listed in Supplementary Table 1.

Agarose 2D-DIGE, GeLC-MS analysis and protein identification

Agarose 2D-DIGE was performed as described previously.[46] In-gel tryptic digestion of proteins and subsequent identification by mass spectrometry was performed as described previously.[46–48]

For GeLC-MS analysis, lanes were excised from SDS–polyacrylamide gel electrophoresis gels using razor blades and cut into 5-mm slices. Digested peptides were introduced from a NanoSpace HPLC (Shiseido Fine Chemicals, Tokyo, Japan) to a LTQ XL (Thermo Scientific, San Jose, CA, USA) ion-trap mass spectrometer via an attached PicoTip (New Objective, Woburn, MA, USA). The Mascot search engine (Matrix Science, London, UK) was used to identify proteins. The minimum criterion of the probability-based MASCOT/MOWSE score was set at a 5% significance threshold level.

Statistics

All data are shown as means ± s.d. Means were compared using the Wilcoxon–Mann–Whitney test. $P < 0.05$ was considered statistically significant in all the calculations. All data analyses were performed using KaleidaGraph version 4.0 (Synergy Software, Reading, PA, USA).

CONFLICT OF INTEREST

The authors declare no conflict of interest.

ACKNOWLEDGEMENTS

We thank Masumi Ishibashi and Nobuko Tanaka for technical assistance. This work was supported by Grants-in-Aid from the Ministry of Education, Science, Sports and Culture of Japan.

REFERENCES

1 Lengauer C, Kinzler KW, Vogelstein B. Genetic instability in colorectal cancers. *Nature* 1997; **386**: 623–627.
2 Lengauer C, Kinzler KW, Vogelstein B. Genetic instabilities in human cancers. *Nature* 1998; **396**: 643–649.
3 Jallepalli PV, Waizenegger IC, Bunz F, Langer S, Speicher MR, Peters JM *et al.* Securin is required for chromosomal stability in human cells. *Cell* 2001; **105**: 445–457.
4 Barber TD, McManus K, Yuen KW, Reis M, Parmigiani G, Shen D *et al.* Chromatid cohesion defects may underlie chromosome instability in human colorectal cancers. *Proc Natl Acad Sci USA* 2008; **105**: 3443–3448.
5 Zhang N, Ge G, Meyer R, Sethi S, Basu D, Pradhan S *et al.* Overexpression of Separase induces aneuploidy and mammary tumorigenesis. *Proc Natl Acad Sci USA* 2008; **105**: 13033–13038.
6 Solomon DA, Kim T, Diaz-Martinez LA, Fair J, Elkahloun AG, Harris BT *et al.* Mutational inactivation of STAG2 causes aneuploidy in human cancer. *Science* 2011; **333**: 1039–1043.
7 Cahill DP, Lengauer C, Yu J, Riggins GJ, Willson JK, Markowitz SD *et al.* Mutations of mitotic checkpoint genes in human cancers. *Nature* 1998; **392**: 300–303.
8 Hanks S, Coleman K, Reid S, Plaja A, Firth H, Fitzpatrick D *et al.* Constitutional aneuploidy and cancer predisposition caused by biallelic mutations in BUB1B. *Nat Genet* 2004; **36**: 1159–1161.
9 Bischoff JR, Anderson L, Zhu Y, Mossie K, Ng L, Souza B *et al.* A homologue of Drosophila aurora kinase is oncogenic and amplified in human colorectal cancers. *EMBO J* 1998; **17**: 3052–3065.
10 Zhou H, Kuang J, Zhong L, Kuo WL, Gray JW, Sahin A *et al.* Tumour amplified kinase STK15/BTAK induces centrosome amplification, aneuploidy and transformation. *Nat Genet* 1998; **20**: 189–193.
11 Ganem NJ, Godinho SA, Pellman D. A mechanism linking extra centrosomes to chromosomal instability. *Nature* 2009; **460**: 278–282.
12 Silkworth WT, Nardi IK, Scholl LM, Cimini D. Multipolar spindle pole coalescence is a major source of kinetochore mis-attachment and chromosome mis-segregation in cancer cells. *PLoS One* 2009; **4**: e6564.
13 Fodde R, Kuipers J, Rosenberg C, Smits R, Kielman M, Gaspar C *et al.* Mutations in the APC tumour suppressor gene cause chromosomal instability. *Nat Cell Biol* 2001; **3**: 433–438.
14 Kaplan KB, Burds AA, Swedlow JR, Bekir SS, Sorger PK, Nathke IS. A role for the Adenomatous Polyposis Coli protein in chromosome segregation. *Nat Cell Biol* 2001; **3**: 429–432.
15 Green RA, Kaplan KB. Chromosome instability in colorectal tumor cells is associated with defects in microtubule plus-end attachments caused by a dominant mutation in APC. *J Cell Biol* 2003; **163**: 949–961.
16 Kops GJ, Foltz DR, Cleveland DW. Lethality to human cancer cells through massive chromosome loss by inhibition of the mitotic checkpoint. *Proc Natl Acad Sci USA* 2004; **101**: 8699–8704.
17 Bakhoum SF, Thompson SL, Manning AL, Compton DA. Genome stability is ensured by temporal control of kinetochore-microtubule dynamics. *Nat Cell Biol* 2009; **11**: 27–35.
18 Bakhoum SF, Genovese G, Compton DA. Deviant kinetochore microtubule dynamics underlie chromosomal instability. *Curr Biol* 2009; **19**: 1937–1942.
19 Tomonaga T, Matsushita K, Yamaguchi S, Oohashi T, Shimada H, Ochiai T *et al.* Overexpression and mistargeting of centromere protein-A in human primary colorectal cancer. *Cancer Res* 2003; **63**: 3511–3516.
20 Tomonaga T, Matsushita K, Ishibashi M, Nezu M, Shimada H, Ochiai T *et al.* Centromere protein H is up-regulated in primary human colorectal cancer and its overexpression induces aneuploidy. *Cancer Res* 2005; **65**: 4683–4689.

21 Kuga T, Nie H, Kazami T, Satoh M, Matsushita K, Nomura F *et al.* Lamin B2 prevents chromosome instability by ensuring proper mitotic chromosome segregation. *Oncogenesis* 2014; **3**: e94.
22 Wang JL, Gray RM, Haudek KC, Patterson RJ. Nucleocytoplasmic lectins. *Biochim Biophys Acta* 2004; **1673**: 75–93.
23 Kumble KD, Iversen PL, Vishwanatha JK. The role of primer recognition proteins in DNA replication: inhibition of cellular proliferation by antisense oligodeoxyribonucleotides. *J Cell Sci* 1992; **101**(Pt 1): 35–41.
24 Vishwanatha JK, Kumble S. Involvement of annexin II in DNA replication: evidence from cell-free extracts of Xenopus eggs. *J Cell Sci* 1993; **105**(Pt 2): 533–540.
25 Esposito I, Penzel R, Chaib-Harrireche M, Barcena U, Bergmann F, Riedl S *et al.* Tenascin C and annexin II expression in the process of pancreatic carcinogenesis. *J Pathol* 2006; **208**: 673–685.
26 Sharma MR, Koltowski L, Ownbey RT, Tuszynski GP, Sharma MC. Angiogenesis-associated protein annexin II in breast cancer: selective expression in invasive breast cancer and contribution to tumor invasion and progression. *Exp Mol Pathol* 2006; **81**: 146–156.
27 Duncan R, Carpenter B, Main LC, Telfer C, Murray GI. Characterisation and protein expression profiling of annexins in colorectal cancer. *Br J Cancer* 2008; **98**: 426–433.
28 Thompson SL, Compton DA. Examining the link between chromosomal instability and aneuploidy in human cells. *J Cell Biol* 2008; **180**: 665–672.
29 Eberhard DA, Karns LR, VandenBerg SR, Creutz CE. Control of the nuclear-cytoplasmic partitioning of annexin II by a nuclear export signal and by p11 binding. *J Cell Sci* 2001; **114**: 3155–3166.
30 Bayani J, Selvarajah S, Maire G, Vukovic B, Al-Romaih K, Zielenska M *et al.* Genomic mechanisms and measurement of structural and numerical instability in cancer cells. *Semin Cancer Biol* 2007; **17**: 5–18.
31 Morency E, Sabra M, Catez F, Texier P, Lomonte P. A novel cell response triggered by interphase centromere structural instability. *J Cell Biol* 2007; **177**: 757–768.
32 Raska I, Andrade LE, Ochs RL, Chan EK, Chang CM, Roos G *et al.* Immunological and ultrastructural studies of the nuclear coiled body with autoimmune antibodies. *Exp Cell Res* 1991; **195**: 27–37.
33 Stoler S, Keith KC, Curnick KE, Fitzgerald-Hayes M. A mutation in CSE4, an essential gene encoding a novel chromatin-associated protein in yeast, causes chromosome nondisjunction and cell cycle arrest at mitosis. *Genes Dev* 1995; **9**: 573–586.
34 Howman EV, Fowler KJ, Newson AJ, Redward S, MacDonald AC, Kalitsis P *et al.* Early disruption of centromeric chromatin organization in centromere protein A (Cenpa) null mice. *Proc Natl Acad Sci USA* 2000; **97**: 1148–1153.
35 Kalitsis P, Fowler KJ, Earle E, Hill J, Choo KH. Targeted disruption of mouse centromere protein C gene leads to mitotic disarray and early embryo death. *Proc Natl Acad Sci USA* 1998; **95**: 1136–1141.
36 Thompson SL, Bakhoum SF, Compton DA. Mechanisms of chromosomal instability. *Curr Biol* 2010; **20**: R285–R295.
37 Tomonaga T, Nomura F. Chromosome instability and kinetochore dysfunction. *Histol Histopathol* 2007; **22**: 191–197.
38 Liu J, Rothermund CA, Ayala-Sanmartin J, Vishwanatha JK. Nuclear annexin II negatively regulates growth of LNCaP cells and substitution of ser 11 and 25 to glu prevents nucleo-cytoplasmic shuttling of annexin II. *BMC Biochem* 2003; **4**: 10.
39 Tomas A, Futter C, Moss SE. Annexin 11 is required for midbody formation and completion of the terminal phase of cytokinesis. *J Cell Biol* 2004; **165**: 813–822.
40 Everett RD, Earnshaw WC, Findlay J, Lomonte P. Specific destruction of kinetochore protein CENP-C and disruption of cell division by herpes simplex virus immediate-early protein Vmw110. *EMBO J* 1999; **18**: 1526–1538.
41 Lomonte P, Everett RD. Herpes simplex virus type 1 immediate-early protein Vmw110 inhibits progression of cells through mitosis and from G(1) into S phase of the cell cycle. *J Virol* 1999; **73**: 9456–9467.
42 Sawyers CL. Research on resistance to cancer drug Gleevec. *Science* 2001; **294**: 1834.
43 Wang TL, Diaz LA Jr, Romans K, Bardelli A, Saha S, Galizia G *et al.* Digital karyotyping identifies thymidylate synthase amplification as a mechanism of resistance to 5-fluorouracil in metastatic colorectal cancer patients. *Proc Natl Acad Sci USA* 2004; **101**: 3089–3094.
44 Chuthapisith S, Layfield R, Kerr ID, Hughes C, Eremin O. Proteomic profiling of MCF-7 breast cancer cells with chemoresistance to different types of anticancer drugs. *Int J Oncol* 2007; **30**: 1545–1551.
45 Takano S, Togawa A, Yoshitomi H, Shida T, Kimura F, Shimizu H *et al.* Annexin II overexpression predicts rapid recurrence after surgery in pancreatic cancer patients undergoing gemcitabine-adjuvant chemotherapy. *Ann Surg Oncol* 2008; **15**: 3157–3168.
46 Nishimori T, Tomonaga T, Matsushita K, Oh-Ishi M, Kodera Y, Maeda T *et al.* Proteomic analysis of primary esophageal squamous cell carcinoma reveals downregulation of a cell adhesion protein, periplakin. *Proteomics* 2006; **6**: 1011–1018.
47 Tomonaga T, Matsushita K, Yamaguchi S, Oh-Ishi M, Kodera Y, Maeda T *et al.* Identification of altered protein expression and post-translational modifications in primary colorectal cancer by using agarose two-dimensional gel electrophoresis. *Clin Cancer Res* 2004; **10**: 2007–2014.
48 Seimiya M, Tomonaga T, Matsushita K, Sunaga M, Oh-Ishi M, Kodera Y *et al.* Identification of novel immunohistochemical tumor markers for primary hepatocellular carcinoma; clathrin heavy chain and formiminotransferase cyclodeaminase. *Hepatology* 2008; **48**: 519–530.

Supplementary Information accompanies this paper on the Oncogene website (http://www.nature.com/onc)

JBC Papers in Press. Published on March 13, 2015 as Manuscript M115.643882
The latest version is at http://www.jbc.org/cgi/doi/10.1074/jbc.M115.643882

Role for tyrosine phosphorylation of A-kinase anchoring protein 8 (AKAP8) in its dissociation from chromatin and the nuclear matrix

Sho Kubota[1], Mariko Morii[1], Ryuzaburo Yuki[1], Noritaka Yamaguchi[1], Hiromi Yamaguchi[1], Kazumasa Aoyama[1], Takahisa Kuga[2], Takeshi Tomonaga[2], and Naoto Yamaguchi[1]

[1]Department of Molecular Cell Biology, Graduate School of Pharmaceutical Sciences, Chiba University, Chiba 260-8675, Japan
[2]Laboratory of Proteome Research, National Institute of Biomedical Innovation, Ibaraki, Osaka 567-0085, Japan

Running title: *Tyrosine phosphorylation of AKAP8*

To whom correspondence should be addressed: Naoto Yamaguchi, Department of Molecular Cell Biology, Graduate School of Pharmaceutical Sciences, Chiba University, Inohana 1-8-1, Chuo-ku, Chiba 260-8675, Japan, Tel & Fax: +81-43-226-2868; E-mail: nyama@faculty.chiba-u.jp

Keywords: Src; A-kinase anchoring protein (AKAP); chromatin remodeling; chromatin; phosphotyrosine signaling; nuclear matrix; AKAP8; nuclear tyrosine phosphorylation signals; chromatin structural changes; global nuclear structure.

Background: Tyrosine kinases are active in the cell nucleus and involved in global nuclear structure.
Results: Phosphorylation of AKAP8 at multiple tyrosine residues by several nucleus-localized tyrosine kinases, including c-Src, induces AKAP8's dissociation from nuclear structures.
Conclusion: Nuclear tyrosine phosphorylation of AKAP8 is involved in global nuclear structure changes.
Significance: These findings highlight the importance of nuclear tyrosine phosphorylation in dynamic chromatin regulation.

ABSTRACT

Protein-tyrosine phosphorylation regulates a wide variety of cellular processes at the plasma membrane. Recently, we showed that nuclear tyrosine kinases induce global nuclear structure changes, which we called chromatin structural changes. However, the mechanisms are not fully understood. In this study, we identify A-kinase anchoring protein 8 (AKAP8/AKAP95), which associates with chromatin and the nuclear matrix, as a nuclear tyrosine-phosphorylated protein. Tyrosine phosphorylation of AKAP8 is induced by several tyrosine kinases, such as Src, Fyn, and c-Abl, but not Syk. Nucleus-targeted Lyn and c-Src strongly dissociate AKAP8 from chromatin and the nuclear matrix in a kinase activity-dependent manner. The levels of tyrosine phosphorylation of AKAP8 are decreased by substitution of multiple tyrosine residues on AKAP8 into phenylalanine. Importantly, the phenylalanine mutations of AKAP8 inhibit its dissociation from nuclear structures, suggesting that the association/dissociation of AKAP8 with/from nuclear structures is regulated by its tyrosine phosphorylation. Furthermore, the phenylalanine mutations of AKAP8 suppress the levels of nuclear tyrosine kinase-induced chromatin structural changes. In contrast, AKAP8 knockdown increases the levels of chromatin structural changes. Intriguingly, stimulation with hydrogen peroxide induces chromatin structural changes, accompanied by the dissociation of AKAP8 from nuclear structures. These results suggest that AKAP8 is involved in the regulation of chromatin structural changes through nuclear tyrosine phosphorylation.

The organization of global nuclear structure

is drastically changed in a wide variety of conditions, such as growth factor stimulation, DNA damage responses, and tumorigenesis. Global nuclear structure changes, which we called chromatin structural changes (1, 2), are involved in regulating gene expression, DNA replication, DNA repair, mitotic progression, and so on (3-6).

Non-receptor tyrosine kinases play important roles in cellular functions, including cell proliferation, adhesion, and differentiation (7, 8). Although tyrosine kinases mainly localize at the cytoplasm and the plasma membrane, they also localize in the nucleus to some extent (9). Src-family tyrosine kinases (SFKs), which are non-receptor-type tyrosine kinases, consist of proto-oncogene products and structurally related proteins, such as c-Src, Lyn, and Fyn (10, 11). We have shown that the members of SFKs localize in the nucleus and induce tyrosine-phosphorylation signals within the nucleus (1, 12-14). c-Abl, a non-receptor-type tyrosine kinase, shuttles between the cytoplasm and the nucleus (2, 15-17). ErbB4, a member of the ErbB family of receptor tyrosine kinases, is cleaved upon ligand stimulation, and the intracellular domain is translocated into the nucleus (18, 19).

Despite the importance of non-receptor-type tyrosine kinases in signal transduction, most studies have focused on their roles as cytoplasmic signaling molecules (7, 8). Recently, nuclear tyrosine kinases were reported to be involved in the regulation of cytoskeletal structures, DNA damage responses, and gene transcription (20-22), although the roles of nuclear tyrosine kinases have not been fully understood. To investigate the role of nuclear tyrosine kinases in chromatin structural changes, we developed a quantitative pixel imaging method with DNA staining of the nucleus (1). Using the pixel imaging method, we have demonstrated that nucleus-localized SFKs and c-Abl induce chromatin structural changes (1, 2). Furthermore, we recently identified KRAB-associated protein 1 (KAP1/TIF1β/TRIM28), which is a component of heterochromatin, as a nuclear substrate of nuclear tyrosine kinases (14). Nuclear tyrosine kinases were found to regulate the function of heterochromatin protein 1α (HP1α), which has important roles in heterochromatin formation, through tyrosine phosphorylation of KAP1 (14). However, the relationship between nuclear tyrosine phosphorylation and chromatin structural changes has not been fully understood.

To further understand the roles for nuclear tyrosine phosphorylation, we recently performed phosphoproteomic analysis of nuclear proteins in HeLa S3 cells expressing nucleus-targeted Lyn or c-Abl (nuclear localization signal (NLS)-fused Lyn and c-Abl). As a result, we identified various nuclear tyrosine-phosphorylated proteins, including A-kinase anchoring protein 8 (AKAP8/AKAP95). AKAP8 is a member of the large family of A-kinase anchoring proteins (AKAPs), which have a common function in binding to protein kinase A (23). AKAP8 was previously shown to be associated with nuclear structures, such as chromatin and the nuclear matrix (24-26). However, it is unclear whether the function of AKAP8 is regulated through a posttranslational modification.

In this study, we examined the roles of tyrosine phosphorylation of AKAP8 in nuclear tyrosine kinase-mediated chromatin structural changes. We showed that AKAP8 is one of the substrates for nuclear tyrosine kinases and tyrosine phosphorylation of AKAP8 at multiple tyrosine residues inhibits its association with nuclear structures. We further showed that tyrosine phosphorylation of AKAP8 is involved in nuclear tyrosine kinase-mediated chromatin structural changes.

EXPERIMENTAL PROCEDURES

Plasmids- Expression vectors for intact c-Src, c-Src (c-Src-HA), and c-Src(KD) were constructed from cDNA encoding human wild-type Src (27) (provided by D. J. Fujita) as described (1, 28). Expression vectors for intact Lyn, NLS-Lyn, and NLS-Lyn-K275A [NLS-Lyn(KD)] were constructed from cDNA encoding human wild-type Lyn (29) (provided by T. Yamamoto) as described (1, 28). An expression vector for intact Fyn was constructed from cDNA encoding human wild-type Fyn (30)

(provided by T. Yamamoto) as described (1, 28). An expression vector for NLS-c-Abl was constructed from cDNA encoding human wild-type c-Abl-1b (c-Abl-wt) (31) (provided by E. Canaani) as described (2). An expression vector for NLS-Syk was constructed from cDNA encoding human wild-type Syk (32) (provided by E. A. Clark) as described (1). An expression vector for NLS-4ICD (ErbB4 intracellular domain) was constructed from cDNA encoding human ErbB4 CYT-1 (33) (provided by S. Yokoyama) as described (19). An expression vector for wild-type AKAP8 tagged with a myc epitope at the N terminus (myc-AKAP8-wt) was constructed from cDNA encoding human wild-type AKAP8. cDNA that encode AKAP8 was generated by PCR from HeLa S3 cell cDNAs with 5'-CTGACGGTACCGCTGGTTCAATGGACC AGGGCTACGGAGGCTACGGG-3' (sense), and 5'-CTAGCTTCTAGATCATTCTGTGGGAAC AGCGTCTTTAGACTCTGCATC-3' (antisense), and the *BamHI-XbaI* fragment of the PCR product was introduced into the *BamHI-XbaI* site of the pcDNA3/myc vector as described (34). The Tyr to Phe mutants of AKAP8 were created by PCR using AKAP8-wt as a template with primers as follows: Y51/53F, 5'-GTCACCACAGGCAGTACTTTCAGCTTC GGCCCAGCCTCGTGGGAG-3' (sense) and 5'-GGCTGGGCCGAAGCTGAAAGTACTGC CTGTGGTGACACTGGTGTTCTG-3' (antisense); Y80F, 5'-TGCCATGCACATGGCTAGCTTCGGCCC AGAGCCATGCACCGAC-3' (sense) and 5'-GGCTCTGGGCCGAAGCTAGCCATGTGC ATGGCAGGGGCCCCGG-3' (antisense); Y146/150/152/154F, 5'-CACAACCCCTTCAGGCCTAGCTTCAGC TTCGACTTTGAGTTCGACCTGG-3' (sense), 5'-GTCGAACTCAAAGTCGAAGCTGAAGCT AGGCCTGAAGGGGTTGTGCTCC-3' (antisense); Y170F, 5'-CAATGGCAGCTTTGGTGGCCAGTTCAG TGAATGCCGAGACCCAGCCC-3' (sense) and 5'-GTCTCGGCATTCACTGAACTGGCCACC AAAGCTGCCATTGCGGTCGGAC-3' (antisense); Y311F, 5'-GGAAACGGAAGCAGTTCCAGCTGTTCG AGGAGCCAGACACCAAACTGG-3' (sense) and 5'-GGTGTCTGGCTCCTCGAACAGCTGGAA CTGCTTCCGTTTCCTGCCCGTG-3' (antisense); Y436F, 5'-GTGGAGTTCCTCCAGGAATTCATTGTA AACAGAAATAAGAAAATTG-3' (sense) and 5'-CTTATTTCTGTTTACAATGAATTCCTGG AGGAACTCCACGGTCTTGTC-3' (antisense); Y539F, 5'-GTGAAGATGCTCGAGAAATTCCTCAAG GGTGAGGACCCTTTCACC-3' (sense) and 5'-CACCCTTGAGGAATTTCTCGAGCATCT TCACTATATGTCTGTTG-3' (antisense).

RNA interference- Knockdown of AKAP8 was performed with short hairpin RNA (shRNA) for silencing AKAP8 (5'-GCCAGGAGCACTTCTTCAA-3') (26). The nucleotides for shRNA were annealed and subcloned into the BglII-XbaI site of the pENTR4/H1 vector (provided by H. Miyoshi) (35, 36). The EBNA1-based episomal pEBMulti-H1 vector, which encodes the H1 promoter and a neomycin-resistant gene, was generated from the pEBMulti vector (Wako Pure Chemical Industries, Osaka, Japan) by replacing the CAG promoter with the H1 promoter, as described (37). The oligonucleotides used for shRNA were annealed and subcloned into the pEBMulti-H1 vector (37-39). To generate AKAP8-knockdown cells, HCT116 cells were transfected with pEBMulti-neo/shAKAP8 selected in 600 μg/ml G418. Viable parental HCT116 cells were not detected after a 5-day selection using 600 μg/ml G418.

Antibodies- The following antibodies were used: phosphotyrosine (pTyr) (4G10 and polyclonal antibody; Upstate Biotechnology, Inc; provided by T. Tamura and T. Yoshimoto) (40), Lyn (Lyn9; Wako Pure Chemical Industries, Osaka, and Lyn44; Santa Cruz Biotechnology), myc (9E10 and polyclonal antibody; Abcam or Santa Cruz Biotechnology), AKAP8 (Millipore or R-146; Santa Cruz Biotechnology), HA (Y11; Santa Cruz Biotechnology), actin (clone C4; CHEMICON International), Syk (4D10; Santa Cruz Biotechnology), Abl (8E9; BD-Pharmingen),

Fyn (Fyn3; Santa Cruz Biotechnology), Src (GD11; Upstate Biotechnology, Inc), ErbB4 (C-18; Santa Cruz Biotechnology), lamin A/C (N-18; Santa Cruz Biotechnology), histone H3 (C-16; Santa Cruz Biotechnology), $cPLA_2$ (4-4B-3C; Santa Cruz Biotechnology). Horseradish peroxidase (HRP)-$F(ab')_2$ secondary antibodies were purchased from Amersham Biosciences. FITC-, and TRITC-labeled IgG secondary antibodies, and Alexa Fluor 488-, Alexa Fluor 546-, and Alexa Fluor 647-labeled IgG secondary antibodies were purchased from BioSource International, Sigma-Aldrich, and Invitrogen.

Cell culture and transfection- HeLa S3 cells (Japanese Collection of Research Bioresources, Osaka), COS-1 cells, and HCT116 cells were cultured in Iscove's modified DME (IMDM) containing 1% fetal bovine serum (FBS) and 4% bovine serum (BS). Cells seeded in a 35-mm (60-mm) culture dish were transiently transfected with 1 μg (3 μg) of plasmid DNA using 5 μg (15 μg) of linear polyethylenimine (25 kDa) (Polyscience, Inc.) (41) or Lipofectamine 2000 (Invitrogen). To inhibit SFK-mediated tyrosine phosphorylation, cells were treated with 10~20 μM PP2 (Sigma) or 10 μM imatinib (LC Laboratories). To induce oxidative stress, cells were treated with 1 mM H_2O_2 at 37°C for 1 h in IMDM.

Western blotting and immunoprecipitation- Cell lysates were prepared in SDS-PAGE sample buffer or Triton X-100 lysis buffer (30 mM HEPES, pH7.4, 100 mM NaCl, 0.5% Triton X-100, 4 mM EDTA, 10 mM NaF, 10 mM Na_3VO_4, 4 μg/ml aprotinin, 4 μg/ml leupeptin, 1.6 μg/ml pepstatin A, and 1 mM phenylmethylsulfonyl fluoride [PMSF]), and subjected to SDS-PAGE and electrotransferred onto PVDF membranes (Millipore). Immunodetection was performed by enhanced chemiluminescence (Millipore), as described (38, 42). Results were analyzed using a ChemiDoc XRS-Plus image analyzer (Bio-Rad). Immunoprecipitation was performed using antibody-precoated protein-G beads, as described (13, 36). The intensity of chemiluminescence was measured using Quantity One software (Bio-Rad). Bars represent means ± S.D. from three independent experiments. Asterisks indicate significant differences (*$p<0.05$, **$p<0.01$) calculated by Student's *t*-test. Composite figures were prepared using GIMP version 2.6.2 and Illustrator version 16.0 (Adobe), as described recently (14). Because two or three independent experiments gave similar results, a representative experiment is shown.

Subcellular fractionation- Cell pellets were washed with phosphate-buffered saline (PBS) and resuspended in 0.2% Triton X-100 extraction buffer (PBS supplemented with 0.2% Triton X-100, 2 mM Na_3VO_4, 4 μg/ml aprotinin, 4 μg/ml leupeptin, 1.6 μg/ml pepstatin A, and 1 mM PMSF) and the cells were kept on ice for 10 min. Soluble fraction was separated by centrifugation at 15,000 x *g* for 10 min. The resulting insoluble fraction was solubilized in SDS sample buffer or 1% Triton X-100 extraction buffer (PBS supplemented with 1% Triton X-100, 2 mM Na_3VO_4, 4 μg/ml aprotinin, 4 μg/ml leupeptin, 1.6 μg/ml pepstatin A, and 1 mM PMSF) and sheared by sonication.

Immunofluorescence- Confocal images were obtained using a Fluoview FV500 confocal laser scanning microscope (Olympus, Tokyo) as described (14, 16). Cells were fixed in PBS containing 4% paraformaldehyde for 20 min. Cells were extracted with 0.2% Triton X-100 extraction buffer for 5 min on ice and fixed in PBS containing 4% paraformaldehyde, or extracted and fixed in PTEMF buffer (20 mM PIPES, pH 6.9, 0.2% Triton X-100, 10 mM EGTA, 1 mM $MgCl_2$, and 4% paraformaldehyde) for 20 min. Cells were permeabilized in PBS containing 0.1% saponin and 3% bovine serum albumin at room temperature. Cells were subsequently reacted with an appropriate primary antibody for 1 h, washed with PBS containing 0.1% saponin, and stained with Alexa Fluor 488-, Alexa Fluor 546-, or Alexa Fluor 647-conjugated secondary antibody for 1 h. For DNA staining, cells were treated with 200 μg/ml RNase A and 20 μg/ml propidium iodide (PI) or TOPRO-3 for 1 h. After staining, cells were mounted in PBS containing 50% glycerol and 1 mg/ml *p*-phenylenediamine. Composite figures were

prepared as described in the 'Western blotting and immunoprecipitation' section (14, 43). For quantitation of amounts of AKAP8, fluorescence intensities of immunostaining were measured using ImageJ software (National Institutes of Health). Bars represent means ± S.D. from a representative experiment. Numbers in parentheses indicate mean values, and asterisks indicate significant differences (*$p<0.05$, **$p<0.01$, ***$p<0.001$) calculated by Student's *t*-test. Scale bars, 10 μm; n, cell number. Because two or three independent experiments gave similar results, a representative experiment is shown.

Quantitation of chromatin structural changes- To quantitate chromatin structural changes, the pixel imaging method that we developed was performed (1, 2). In brief, confocal images of PI-stained nuclei were obtained as described above. PI fluorescence intensity of each pixel was quantitated using ImageJ software. The level of chromatin structural changes was represented by the S.D. value for each cell under conditions where the mean value of fluorescence intensity per pixel for each cell ranged between 2500 and 2900. Two-dimensional (2D) plot analyses were performed with S.D. values of PI intensity versus mean fluorescence intensity of anti-AKAP8 antibody.

RESULTS

Tyrosine phosphorylation of AKAP8- To identify the tyrosine-phosphorylated proteins in the nucleus, we established cell lines that express either Lyn tyrosine kinase tagged with a nuclear localization signal (NLS-Lyn) or c-Abl tyrosine kinase tagged with a nuclear localization signal (NLS-c-Abl). Nuclear tyrosine-phosphorylated proteins were purified with anti-pTyr antibody as recently reported (14, 16, 34). We identified the nuclear structure-binding protein AKAP8 as a candidate substrate of nuclear tyrosine kinases. To validate tyrosine phosphorylation of AKAP8, we cotransfected cells with myc-tagged AKAP8 (myc-AKAP8-wt) plus NLS-Lyn or myc-AKAP8-wt plus NLS-Lyn(kinase-dead, KD) in the presence or absence of the SFK inhibitor PP2 and subjected to immunoprecipitation and Western blotting analysis. myc-AKAP8-wt was tyrosine-phosphorylated by NLS-Lyn but not NLS-Lyn(KD), and PP2 treatment inhibited tyrosine phosphorylation of myc-AKAP8-wt (Fig. 1A). Next, to examine which SFK members dominantly phosphorylate AKAP8, we cotransfected cells with myc-AKAP-wt plus intact c-Src, intact Lyn, or intact Fyn. Expression of c-Src was found to strongly induce tyrosine phosphorylation of AKAP8 among SFKs (Fig. 1B). Our previous studies showed that several tyrosine kinases, including SFKs and c-Abl, except for Syk, located in the nucleus are involved in induction of chromatin structural changes (1, 2, 19). Interestingly, AKAP8 was tyrosine-phosphorylated by not only NLS-Lyn but also NLS-c-Abl and NLS-4ICD (NLS-tagged ErbB4 intracellular domain), but was not by NLS-Syk (Fig. 1C). These results suggest that AKAP8 is tyrosine-phosphorylated by some nuclear tyrosine kinases, such as SFKs, c-Abl, and 4ICD.

Effect of tyrosine phosphorylation of AKAP8 on its association with nuclear structures- To elucidate the role of tyrosine phosphorylation in AKAP8 localization, we examined whether NLS-Lyn expression affected the localization of AKAP8 in the nucleus. Expression of NLS-Lyn diffusely delocalized endogenous AKAP8 in the nucleus, whereas endogenous AKAP8 in control cells appeared to be localized to some nuclear structures, suggesting that NLS-Lyn expression changes the localization of AKAP8 in the nucleus (Fig. 2A). Notably, neither expression of NLS-Lyn(KD) nor inhibition of NLS-Lyn by PP2 did induce delocalization of AKAP8 (Fig. 2A). Considering that AKAP8 is associated with the nuclear matrix and chromatin (24), these results raise the intriguing possibility that tyrosine phosphorylation of AKAP8 is capable of dissociating AKAP8 from nuclear structures, e.g. the nuclear matrix and chromatin.

To examine the effect of tyrosine phosphorylation of AKAP8 on its association with nuclear structures, cells were transfected

with NLS-Lyn, extracted with 0.2% Triton X-100 extraction buffer, and stained for AKAP8. Without extraction, the levels of AKAP8 were not changed irrespective of NLS-Lyn expression. Intriguingly, the levels of Triton X-100-insoluble AKAP8 were drastically decreased in NLS-Lyn-expressing cells compared to control cells (Fig. 2B). Expression of wild-type c-Src, which is present in the nucleus to a considerable extent, also decreased the amounts of Triton X-100-insoluble AKAP8 (Fig. 2C). These results suggest that nuclear SFKs are involved in dissociation of AKAP8 from nuclear structures. To further ascertain the effect of tyrosine phosphorylation on AKAP8's dissociation from nuclear structures, cells were subfractionated into Triton X-100-soluble and insoluble fractions. Triton-X-100-insoluble fraction contained the chromatin protein histone H3 and the nuclear lamina protein lamin A/C (Fig. 2D). Western blotting analyses showed that the amounts of endogenous AKAP8 present in insoluble fraction were decreased upon NLS-Lyn expression (Fig. 2D, E). However, NLS-Lyn(KD) expression decreased the amounts of endogenous AKAP8 in insoluble fraction, and PP2 treatment inhibited the decrease in the amounts of endogenous AKAP8 present in insoluble fraction upon NLS-Lyn expression (Fig. 2E).

Next, we cotransfected cells with myc-AKAP8-wt plus NLS-Lyn, subsequently extracted with 0.2% Triton X-100 extraction buffer, and stained for AKAP8. Consistent with endogenous AKAP8 (Fig. 2B), the levels of Triton X-100-insoluble myc-AKAP8-wt were drastically decreased upon NLS-Lyn expression (Fig. 2F). Subcellular fractionation experiments showed that expression of NLS-Lyn or c-Src decreased the amounts of myc-AKAP8-wt in Triton X-100-insoluble fraction in a kinase activity-dependent manner (Fig. 2G, H). Importantly, the tyrosine phosphorylation levels of myc-AKAP8-wt in Triton X-100-soluble fraction were much higher than those in Triton X-100-insoluble fraction (Fig. 2I). Furthermore, we examined whether endogenous SFKs' activity affected the association of endogenous AKAP8 with nuclear structures, and found that treatment of HCT116 cells, which highly express endogenous c-Src, with PP2 increased the amounts of AKAP8 in Triton X-100-insoluble fraction compared to that with control or the Abl inhibitor imatinib (Fig. 2J). Taken together, these results indicate that tyrosine phosphorylation of AKAP8 by SFKs in the nucleus is capable of dissociating AKAP8 from nuclear structures.

Dissociation of AKAP8 from nuclear structures through phosphorylation of its multiple tyrosine residues- We detected tyrosine-phosphorylated peptides of AKAP8-pTyr-311 (307-QFQLpYEEPDTK-317) and AKAP8-pTyr-436 (425-LPDKTCEFLQEpYIVNR-440) by mass spectrometry. In the PhosphoSitePlus proteomics database, phosphorylation of AKAP8 at Tyr-150, Tyr-154, Tyr-170, and Tyr-311 are listed (44). A previous phosphoproteomic study showed that Tyr-152 was phosphorylated upon PDGF stimulation (45). Taken together, we speculated that AKAP8 might be phosphorylated at multiple tyrosine residues by nuclear tyrosine kinases.

To identify tyrosine phosphorylation sites of AKAP8 that could affect the localization of AKAP8, we constructed several YF mutants, which are mutated tyrosine to phenylalanine (Fig. 3A). We then cotransfected cells with myc-AKAP8-wt plus NLS-Lyn or its YF mutant plus NLS-Lyn, extracted with 0.2% Triton X-100 extraction buffer, and stained for myc-AKAP8-wt or -mutant. 4CYF mutations (Y170F, Y311F, Y436F, and Y539F), including the tyrosine phosphorylation sites that we detected, did not inhibit dissociation of AKAP8 from nuclear structures (Fig. 3B). However, 5NYF mutations (Y146F, Y150F, Y152F, Y154F, and Y170F) and 8NYF mutations (Y51F, Y53F, Y80F, Y146F, Y150F, Y152F, Y154F, and Y170F) only partially inhibited dissociation of AKAP8 from nuclear structures upon NLS-Lyn expression (Fig. 3C, D). Notably, we found that 11YF mutations (Y51F, Y53F, Y80F, Y146F, Y150F, Y152F, Y154F, Y170F, Y311F, Y436F, and Y539F) strongly inhibited dissociation of AKAP8 from nuclear structures upon NLS-Lyn expression (Fig. 4A, B, C).

Next, to examine whether these tyrosine residues are indeed tyrosine phosphorylation sites of AKAP8, we cotransfected cells with myc-AKAP8-wt plus NLS-Lyn or its YF mutants plus NLS-Lyn. NLS-Lyn-induced tyrosine phosphorylation levels of myc-AKAP8-4CYF, -5NYF, and -8NYF were partially decreased compared with myc-AKAP8-wt (Fig. 3E). Nevertheless, NLS-Lyn-induced tyrosine phosphorylation levels of myc-AKAP8-11YF were decreased to 44% of that of myc-AKAP8-wt (Fig. 4D). Similar results were obtained by cotransfection with myc-AKAP8-11YF plus c-Src (Fig. 4E). Taken together, these results suggest that AKAP8 can dissociate from nuclear structures when its multiple tyrosine residues are phosphorylated by nuclear tyrosine kinases.

Involvement of tyrosine-phosphorylated AKAP8 in chromatin structural changes- We previously showed that SFKs induce chromatin structural changes (1). Our pixel imaging method showed a positive correlation between the S.D. values of PI fluorescence intensity and the levels of chromatin structural changes (1, 2). Thus, we examined whether there was a relationship between the S.D. values of PI fluorescence intensity of chromatin and the levels of AKAP8 association with nuclear structures. Consistent with our previous study (1), NLS-Lyn induced strong chromatin structural changes compared to control vector and NLS-Lyn(KD) (Fig. 5A). 2D-plot analyses showed that there was a strong inverse correlation between the levels of Triton X-100-insoluble AKAP8 and chromatin structural changes in NLS-Lyn-expressing cells but not NLS-Lyn(KD)-expressing cells (Fig. 5A). Similar to NLS-Lyn, the levels of Triton X-100-insoluble AKAP8 inversely correlated with chromatin structural changes in c-Src-expressing cells, but not c-Src(KD)-expressing cells (Fig. 5B). These results indicate that the dissociation of AKAP8 from nuclear structures is positively correlated with nuclear tyrosine phosphorylation-mediated chromatin structural changes.

To examine whether the dissociation of AKAP8 from nuclear structures induced by nuclear tyrosine kinases is involved in tyrosine phosphorylation-mediated chromatin structural changes, we cotransfected cells with NLS-Lyn plus myc-AKAP8-wt or NLS-Lyn plus myc-AKAP8-11YF. The levels of chromatin structural changes induced by NLS-Lyn in myc-AKAP8-11YF-expressing cells were significantly lower than those in myc-AKAP8-wt-expressing cells (Fig. 6A). Furthermore, we examined the effect of AKAP8-knockdown on chromatin structural changes. The levels of chromatin structural changes in AKAP8-knockdown cells were higher than those in control cells (Fig. 6B, C). These results suggest that the dissociation of AKAP8 from nuclear structures is involved in chromatin structural changes induced by nuclear tyrosine phosphorylation.

Oxidative stress activates tyrosine kinases, including SFKs (46-48), and affects gene transcription, epigenetic regulation and regulation of global nuclear structure (49, 50). Also, we showed that treatment with H_2O_2 induces activation of SFKs and chromatin structural changes (1, 51). Therefore, we examined the effect of oxidative stress on the association of AKAP8 with nuclear structures. Consistent with our previous study (1), H_2O_2 treatment induced chromatin structural changes, which were inhibited in part by PP2 treatment (Fig. 6D). Importantly, by examining Triton X-100-insoluble fractions, we found that H_2O_2 treatment induced the dissociation of endogenous AKAP8 from nuclear structures and its dissociation was inhibited in part by PP2 treatment (Fig. 6D, E). These results suggest that oxidative stress-induced chromatin structural changes involve the dissociation of endogenous AKAP8 from nuclear structures through SFK activation.

DISCUSSION

Although AKAP8 is known to associate with nuclear structures, such as the nuclear matrix and chromatin, and act as a scaffolding protein (24-26), it has thus far not been reported that the interaction of AKAP8 with nuclear structures is regulated through posttranslational modifications. In the present study, we show

that AKAP8 can dissociate from nuclear structures through its tyrosine phosphorylation mediated by nuclear c-Src and that the dissociation of AKAP8 is involved in global nuclear structure changes, which we called chromatin structural changes (1, 2).

Many studies have shown the functions of serine/threonine kinases present in the nucleus (4, 6, 52). However, a limited number of studies showed the functions of the tyrosine kinases present in the nucleus (1, 2, 12, 14, 22, 53, 54). Since tyrosine kinases are largely located at the plasma membrane and the cytoplasm, tyrosine phosphorylation signals have been hardly detected in the nucleus. Nonetheless, carefully using a high dose of the potent tyrosine phosphatase inhibitor Na_3VO_4, we were eventually able to detect tyrosine phosphorylation of nuclear proteins (1, 2, 12-14, 16, 19, 34, 53, 55). Given that tyrosine phosphatases are abundant in the nucleus (9), we assume that, like ON/OFF switching in a microprocessor, phosphorylation levels of nuclear proteins may be very rapidly regulated by a balance between the activity of nuclear tyrosine kinases and that of nuclear tyrosine phosphatases (1, 14, 34). To understand the role of nuclear tyrosine phosphorylation, we created nucleus-targeted tyrosine kinases and transfected them into cells. As a result, many unidentified nuclear proteins were found to be tyrosine-phosphorylated (1, 2). Our recent study showed that tyrosine phosphorylation of KAP1, which is one of the nuclear substrates that we found, induces the dissociation of KAP1 and HP1α from heterochromatin (14). Our findings in this study also shows that tyrosine phosphorylation of AKAP8, another nuclear protein, induces its dissociation from nuclear structures (Figs. 1~4). Collectively, some of the tyrosine kinases that are present in the nucleus may be involved in the regulation of the interaction of their nuclear substrates with chromatin and the nuclear matrix through tyrosine phosphorylation of their nuclear substrates *per se*.

We have been studying the functional commonalities and differences among nuclear tyrosine kinases (1, 2, 12, 14, 19, 53). Our results showed that NLS-Lyn induces tyrosine phosphorylation of AKAP8 much stronger than intact Lyn (Fig. 1A, B), suggesting that nuclear Lyn is important for tyrosine phosphorylation of AKAP8. In contrast to Lyn, intact c-Src strongly induces phosphorylation of AKAP8 at tyrosine residues (Fig. 1B). Considering that c-Src induces high levels of phosphorylation of nuclear proteins, including KAP1, compared with the other SFK members (14), it is likely that, among SFKs, c-Src in particular plays an important role in tyrosine phosphorylation signaling in the nucleus. Alternatively, it is conceivable that the levels of tyrosine phosphorylation of the nuclear SFK substrates are attributable to the substrate specificity of individual SFKs, because Fyn induces tyrosine phosphorylation of AKAP8 but not KAP1 (Fig. 1B; see also ref. 14).

Previous studies showed that the nuclear matrix-targeted sequence (NMTS) (amino acids 110~140) on AKAP8 is determined for the association of AKAP8 with the nuclear matrix (24). AKAP8 has also been shown to be recruited to mitotic chromosomes via the residues 387~450, including the zinc-finger domain, and to play a role in mitotic progression (25, 26). Because the phosphorylation sites of AKAP8 at Tyr-51, -53, -80, -146, -150, -152, -154, and -170 are located close to the NMTS and those at Tyr-311, -436, and -527 are located close to the zinc-finger domain (Figs. 3A, 4A), we hypothesize that phosphorylation at those tyrosine residues may interfere with the association of AKAP8 with the nuclear matrix and chromatin. In addition, AKAP8 is known to associate with the histone modification enzyme MLL2 complex via the N-terminal region of AKAP8 and regulate transcription in embryonic stem cells (56). Phosphorylation of AKAP8 at Tyr-51, -53, and -80 might be involved in MLL2-driven transcription in embryonic stem cells, because we showed that tyrosine phosphorylation-mediated chromatin structural changes lead to histone modifications and gene transcription (2, 19). Generation of AKAP8-YF knock-in embryonic stem cells might enable us to investigate an *in vivo* role of tyrosine phosphorylation of AKAP8 in transcription

during development.

Chromatin structural changes are involved in gene expression, DNA replication, mitotic progression, and so on (1, 3-5). It is evident that AKAP8 knockdown significantly induces chromatin structural changes (Fig. 6B, C), although the levels of chromatin structural changes were relatively low upon AKAP8 knockdown compared to those induced by expression of nuclear tyrosine kinases. Furthermore, oxidative stress induces chromatin structural changes, at least in part, by dissociating AKAP8 from nuclear structures through SFK activation (Fig. 6D). In addition, the association of AKAP8 with nuclear structures is involved in gene expression, DNA replication, and mitotic progression (26, 56, 57). Recently, the nuclear proteins KAT5, histone H4, and HDAC2 were reported to be tyrosine-phosphorylated and to functionally associate with chromatin structures (22, 54, 58). Taken together, we assume that tyrosine phosphorylation of various nuclear proteins, including AKAP8, is attributable to nuclear tyrosine kinase-mediated chromatin structural changes, which could be involved in a variety of nuclear function, such as gene expression, DNA replication, mitotic progression.

In conclusion, we identify AKAP8 as a nuclear substrate of nuclear tyrosine kinases. Although tyrosine phosphorylation of AKAP8 has been already reported, this is a first report of functional regulation of AKAP8 through its tyrosine phosphorylation. Multiple tyrosine phosphorylation of AKAP8 is involved in its dissociation from nuclear structures, leading to chromatin structural changes. Further studies will help us to deeply understand the relationship between nuclear tyrosine phosphorylation and chromatin structure.

REFERENCES

1. Takahashi, A., Obata, Y., Fukumoto, Y., Nakayama, Y., Kasahara, K., Kuga, T., Higashiyama, Y., Saito, T., Yokoyama, K. K., and Yamaguchi, N. (2009) Nuclear localization of Src-family tyrosine kinases is required for growth factor-induced euchromatinization. *Exp. Cell Res.* **315**, 1117-1141
2. Aoyama, K., Fukumoto, Y., Ishibashi, K., Kubota, S., Morinaga, T., Horiike, Y., Yuki, R., Takahashi, A., Nakayama, Y., and Yamaguchi, N. (2011) Nuclear c-Abl-mediated tyrosine phosphorylation induces chromatin structural changes through histone modifications that include H4K16 hypoacetylation. *Exp. Cell Res.* **317**, 2874-2903
3. Nowak, S. J., and Corces, V. G. (2004) Phosphorylation of histone H3: a balancing act between chromosome condensation and transcriptional activation. *Trends Genet.* **20**, 214-220
4. Kouzarides, T. (2007) Chromatin modifications and their function. *Cell* **128**, 693-705
5. Méchali, M. (2010) Eukaryotic DNA replication origins: many choices for appropriate answers. *Nat. Rev. Mol. Cell Biol.* **11**, 728-738
6. Shiloh, Y., and Ziv, Y. (2013) The ATM protein kinase: regulating the cellular response to genotoxic stress, and more. *Nat. Rev. Mol. Cell Biol.* **14**, 197-210
7. Hubbard, S. R., and Till, J. H. (2000) Protein tyrosine kinase structure and function. *Annu. Rev. Biochem.* **69**, 373-398
8. Hunter, T. (2009) Tyrosine phosphorylation: thirty years and counting. *Curr. Opin. Cell Biol.* **21**, 140-146
9. Cans, C., Mangano, R., Barilá, D., Neubauer, G., and Superti-Furga, G. (2000) Nuclear tyrosine phosphorylation: the beginning of a map. *Biochem. Pharmacol.* **60**, 1203-1215
10. Thomas, S. M., and Brugge, J. S. (1997) Cellular functions regulated by Src family kinases. *Annu. Rev. Cell Dev. Biol.* **13**, 513-609
11. Reynolds, A. B., Kanner, S. B., Bouton, A. H., Schaller, M. D., Weed, S. A., Flynn, D. C., and Parsons, J. T. (2014) SRChing for the substrates of Src. *Oncogene* **33**, 4537-4547
12. Yamaguchi, N., Nakayama, Y., Urakami, T., Suzuki, S., Nakamura, T., Suda, T., and Oku, N. (2001) Overexpression of the Csk homologous kinase (Chk tyrosine kinase) induces multinucleation: a possible role for chromosome-associated Chk in chromosome dynamics. *J. Cell Sci.* **114**, 1631-1641
13. Ikeda, K., Nakayama, Y., Togashi, Y., Obata, Y., Kuga, T., Kasahara, K., Fukumoto, Y., and Yamaguchi, N. (2008) Nuclear localization of Lyn tyrosine kinase mediated by inhibition of its kinase activity. *Exp. Cell Res.* **314**, 3392-3404
14. Kubota, S., Fukumoto, Y., Aoyama, K., Ishibashi, K., Yuki, R., Morinaga, T., Honda, T., Yamaguchi, N., Kuga, T., Tomonaga, T., and Yamaguchi, N. (2013) Phosphorylation of KRAB-associated protein 1 (KAP1) at Tyr-449, Tyr-458, and Tyr-517 by nuclear tyrosine kinases inhibits the association of KAP1 and heterochromatin protein 1α (HP1α) with heterochromatin. *J. Biol. Chem.* **288**, 17871-17883
15. Taagepera, S., McDonald, D., Loeb, J. E., Whitaker, L. L., McElroy, A. K., Wang, J. Y., and Hope, T. J. (1998) Nuclear-cytoplasmic shuttling of C-ABL tyrosine kinase. *Proc. Natl. Acad. Sci. U.S.A.* **95**, 7457-7462
16. Aoyama, K., Yuki, R., Horiike, Y., Kubota, S., Yamaguchi, N., Morii, M., Ishibashi, K., Nakayama, Y., Kuga, T., Hashimoto, Y., Tomonaga, T., and Yamaguchi, N. (2013) Formation of long and winding nuclear F-actin bundles by nuclear c-Abl tyrosine kinase. *Exp. Cell Res.* **319**, 3251-3268
17. Greuber, E. K., Smith-Pearson, P., Wang, J., and Pendergast, A. M. (2013) Role of ABL family kinases in cancer: from leukaemia to solid tumours. *Nat. Rev. Cancer* **13**, 559-571
18. Ni, C. Y., Murphy, M. P., Golde, T. E., and Carpenter, G. (2001) gamma-Secretase cleavage and nuclear localization of ErbB-4 receptor tyrosine kinase. *Science* **294**, 2179-2181
19. Ishibashi, K., Fukumoto, Y., Hasegawa, H., Abe, K., Kubota, S., Aoyama, K., Nakayama, Y., and Yamaguchi, N. (2013) Nuclear ErbB4 signaling through H3K9me3 is antagonized by

EGFR-activated c-Src. *J. Cell Sci.* **126**, 625-637
20. Chellappa, K., Jankova, L., Schnabl, J. M., Pan, S., Brelivet, Y., Fung, C. L., Chan, C., Dent, O. F., Clarke, S. J., Robertson, G. R., and Sladek, F. M. (2012) Src tyrosine kinase phosphorylation of nuclear receptor HNF4α correlates with isoform-specific loss of HNF4α in human colon cancer. *Proc. Natl. Acad. Sci. U.S.A.* **109**, 2302-2307
21. Guilluy, C., Osborne, L. D., Van Landeghem, L., Sharek, L., Superfine, R., Garcia-Mata, R., and Burridge, K. (2014) Isolated nuclei adapt to force and reveal a mechanotransduction pathway in the nucleus. *Nat. Cell Biol.* **16**, 376-381
22. Kaidi, A., and Jackson, S. P. (2013) KAT5 tyrosine phosphorylation couples chromatin sensing to ATM signalling. *Nature* **498**, 70-74
23. Wong, W., and Scott, J. D. (2004) AKAP signalling complexes: focal points in space and time. *Nat. Rev. Mol. Cell Biol.* **5**, 959-970
24. Akileswaran, L., Taraska, J. W., Sayer, J. A., Gettemy, J. M., and Coghlan, V. M. (2001) A-kinase-anchoring protein AKAP95 is targeted to the nuclear matrix and associates with p68 RNA helicase. *J. Biol. Chem.* **276**, 17448-17454
25. Eide, T., Carlson, C., Taskén, K. A., Hirano, T., Taskén, K., and Collas, P. (2002) Distinct but overlapping domains of AKAP95 are implicated in chromosome condensation and condensin targeting. *EMBO Rep.* **3**, 426-432
26. Li, Y., Kao, G. D., Garcia, B. A., Shabanowitz, J., Hunt, D. F., Qin, J., Phelan, C., and Lazar, M. A. (2006) A novel histone deacetylase pathway regulates mitosis by modulating Aurora B kinase activity. *Genes. Dev.* **20**, 2566-2579
27. Bjorge, J. D., Bellagamba, C., Cheng, H. C., Tanaka, A., Wang, J. H., and Fujita, D. J. (1995) Characterization of two activated mutants of human pp60c-src that escape c-Src kinase regulation by distinct mechanisms. *J. Biol. Chem.* **270**, 24222-24228
28. Sato, I., Obata, Y., Kasahara, K., Nakayama, Y., Fukumoto, Y., Yamasaki, T., Yokoyama, K. K., Saito, T., and Yamaguchi, N. (2009) Differential trafficking of Src, Lyn, Yes and Fyn is specified by the state of palmitoylation in the SH4 domain. *J. Cell Sci.* **122**, 965-975
29. Yamanashi, Y., Fukushige, S., Semba, K., Sukegawa, J., Miyajima, N., Matsubara, K., Yamamoto, T., and Toyoshima, K. (1987) The yes-related cellular gene lyn encodes a possible tyrosine kinase similar to p56lck. *Mol. Cell. Biol.* **7**, 237-243
30. Tezuka, T., Umemori, H., Akiyama, T., Nakanishi, S., and Yamamoto, T. (1999) PSD-95 promotes Fyn-mediated tyrosine phosphorylation of the N-methyl-D-aspartate receptor subunit NR2A. *Proc. Natl. Acad. Sci. U.S.A.* **96**, 435-440
31. Shtivelman, E., Lifshitz, B., Gale, R. P., and Canaani, E. (1985) Fused transcript of abl and bcr genes in chronic myelogenous leukaemia. *Nature* **315**, 550-554
32. Law, C. L., Sidorenko, S. P., Chandran, K. A., Draves, K. E., Chan, A. C., Weiss, A., Edelhoff, S., Disteche, C. M., and Clark, E. A. (1994) Molecular cloning of human Syk. A B cell protein-tyrosine kinase associated with the surface immunoglobulin M-B cell receptor complex. *J. Biol. Chem.* **269**, 12310-12319
33. Ogiso, H., Ishitani, R., Nureki, O., Fukai, S., Yamanaka, M., Kim, J. H., Saito, K., Sakamoto, A., Inoue, M., Shirouzu, M., and Yokoyama, S. (2002) Crystal structure of the complex of human epidermal growth factor and receptor extracellular domains. *Cell* **110**, 775-787
34. Aoyama, K., Yamaguchi, N., Yuki R., Morii, M., Kubota, S., Hirata, K., Abe, K., Honda, T., Kuga, T., Hashimoto, Y., Tomonaga, T., and Yamaguchi N. (2015) c-Abl induces stabilization of histone deacetylase 1 (HDAC1) in a kinase activity-dependent manner. *Cell Biol. Int.*, in press. doi: 10.1002/cbin.10413
35. Nakayama, Y., Igarashi, A., Kikuchi, I., Obata, Y., Fukumoto, Y., and Yamaguchi, N. (2009) Bleomycin-induced over-replication involves sustained inhibition of mitotic entry through the ATM/ATR pathway. *Exp. Cell Res.* **315**, 2515-2528
36. Obata, Y., Fukumoto, Y., Nakayama, Y., Kuga, T., Dohmae, N., and Yamaguchi, N. (2010) The Lyn kinase C-lobe mediates Golgi export of Lyn through conformation-dependent ACSL3

association. *J. Cell Sci.* **123**, 2649-2662

37. Hasegawa, H., Ishibashi, K., Kubota, S., Yamaguchi, C., Yuki, R., Nakajo, H., Eckner, R., Yamaguchi, N., Yokoyama, K. K., and Yamaguchi, N. (2014) Cdk1-mediated phosphorylation of human ATF7 at Thr-51 and Thr-53 promotes cell-cycle progression into M phase. *PLoS One* **9**, e116048
38. Kubota, S., Fukumoto, Y., Ishibashi, K., Soeda, S., Kubota, S., Yuki, R., Nakayama, Y., Aoyama, K., Yamaguchi, N., and Yamaguchi, N. (2014) Activation of the prereplication complex is blocked by mimosine through reactive oxygen species-activated ataxia telangiectasia mutated (ATM) protein without DNA damage. *J. Biol. Chem.* **289**, 5730-5746
39. Yuki, R., Aoyama, K., Kubota, S., Yamaguchi, N., Kubota, S., Hasegawa, H., Morii, M., Huang, X., Liu, K., Williams, R., Fukuda, M. N., and Yamaguchi, N. (2015) Overexpression of Zinc-finger protein 777 (ZNF777) inhibits proliferation at low cell density through down-regulation of FAM129A. *J. Cell Biochem.*, in press. doi: 10.1002/jcb.25046
40. Tamura, T., Kunimatsu, T., Yee, S. T., Igarashi, O., Utsuyama, M., Tanaka, S., Miyazaki, S., Hirokawa, K., and Nariuchi, H. (2000) Molecular mechanism of the impairment in activation signal transduction in CD4(+) T cells from old mice. *Int. Immunol.* **12**, 1205-1215
41. Fukumoto, Y., Obata, Y., Ishibashi, K., Tamura, N., Kikuchi, I., Aoyama, K., Hattori, Y., Tsuda, K., Nakayama, Y., and Yamaguchi, N. (2010) Cost-effective gene transfection by DNA compaction at pH 4.0 using acidified, long shelf-life polyethylenimine. *Cytotechnology* **62**, 73-82
42. Kasahara, K., Nakayama, Y., Ikeda, K., Fukushima, Y., Matsuda, D., Horimoto, S., and Yamaguchi, N. (2004) Trafficking of Lyn through the Golgi caveolin involves the charged residues on alphaE and alphaI helices in the kinase domain. *J. Cell Biol.* **165**, 641-652
43. Soeda, S., Nakayama, Y., Honda, T., Aoki, A., Tamura, N., Abe, K., Fukumoto, Y., and Yamaguchi, N. (2013) v-Src causes delocalization of Mklp1, Aurora B, and INCENP from the spindle midzone during cytokinesis failure. *Exp. Cell Res.* **319**, 1382-1397
44. Hornbeck, P. V., Kornhauser, J. M., Tkachev, S., Zhang, B., Skrzypek, E., Murray, B., Latham, V., and Sullivan, M. (2012) PhosphoSitePlus: a comprehensive resource for investigating the structure and function of experimentally determined post-translational modifications in man and mouse. *Nucleic Acids Res.* **40**, D261-270
45. Amanchy, R., Zhong, J., Molina, H., Chaerkady, R., Iwahori, A., Kalume, D. E., Grønborg, M., Joore, J., Cope, L., and Pandey, A. (2008) Identification of c-Src tyrosine kinase substrates using mass spectrometry and peptide microarrays. *J. Proteome Res.* **7**, 3900-3910
46. Hardwick, J. S., and Sefton, B. M. (1995) Activation of the Lck tyrosine protein kinase by hydrogen peroxide requires the phosphorylation of Tyr-394. *Proc. Natl. Acad. Sci. U.S.A.* **92**, 4527-4531
47. Sun, X., Majumder, P., Shioya, H., Wu, F., Kumar, S., Weichselbaum, R., Kharbanda, S., and Kufe, D. (2000) Activation of the cytoplasmic c-Abl tyrosine kinase by reactive oxygen species. *J. Biol. Chem.* **275**, 17237-17240
48. Chan, H. L., Chou, H. C., Duran, M., Gruenewald, J., Waterfield, M. D., Ridley, A., and Timms, J. F. (2010) Major role of epidermal growth factor receptor and Src kinases in promoting oxidative stresss-dependent loss of adhesion and apoptosis in epithelial cells. *J. Biol. Chem.* **285**, 4307-4318
49. Cencioni, C., Spallotta, F., Martelli, F., Valente, S., Mai, A., Zeiher, A. M., and Gaetano, C. (2013) Oxidative stress and epigenetic regulation in ageing and age-related diseases. *Int. J. Mol. Sci.* **14**, 17643-17663
50. Sundar, I. K., Yao, H., and Rahman, I. (2013) Oxidative stress and chromatin remodeling in chronic obstructive pulmonary disease and smoking-related diseases. *Antioxid. Redox Signal.* **18**, 1956-1971
51. Matsuda, D., Nakayama, Y., Horimoto, S., Kuga, T., Ikeda, K., Kasahara, K., and Yamaguchi, N. (2006) Involvement of Golgi-associated Lyn tyrosine kinase in the translocation of annexin II

to the endoplasmic reticulum under oxidative stress. *Exp. Cell Res.* **312**, 1205-1217
52. Nishibuchi, G., Machida, S., Osakabe, A., Murakoshi, H., Hiragami-Hamada, K., Nakagawa, R., Fischle, W., Nishimura, Y., Kurumizaka, H., Tagami, H., and Nakayama, J. (2014) N-terminal phosphorylation of HP1α increases its nucleosome-binding specificity. *Nucleic Acids Res.* **42**, 12498-12511
53. Nakayama, Y., Kawana, A., Igarashi, A., and Yamaguchi, N. (2006) Involvement of the N-terminal unique domain of Chk tyrosine kinase in Chk-induced tyrosine phosphorylation in the nucleus. *Exp. Cell Res.* **312**, 2252-2263
54. Gonzalez-Zuñiga, M., Contreras, P. S., Estrada, L. D., Chamorro, D., Villagra, A., Zanlungo, S., Seto, E., and Alvarez, A. R. (2014) c-Abl stabilizes HDAC2 levels by tyrosine phosphorylation repressing neuronal gene expression in Alzheimer's disease. *Mol. Cell* **56**, 163-173
55. Nakayama, Y., and Yamaguchi, N. (2005) Multi-lobulation of the nucleus in prolonged S phase by nuclear expression of Chk tyrosine kinase. *Exp. Cell Res.* **304**, 570-581
56. Jiang, H., Lu, X., Shimada, M., Dou, Y., Tang, Z., and Roeder, R. G. (2013) Regulation of transcription by the MLL2 complex and MLL complex-associated AKAP95. *Nat. Struct. Mol. Biol.* **20**, 1156-1163
57. Eide, T., Taskén, K. A., Carlson, C., Williams, G., Jahnsen, T., Taskén, K., and Collas, P. (2003) Protein kinase A-anchoring protein AKAP95 interacts with MCM2, a regulator of DNA replication. *J. Biol. Chem.* **278**, 26750-26756
58. Chou, R. H., Wang, Y. N., Hsieh, Y. H., Li, L. Y., Xia, W., Chang, W. C., Chang, L. C., Cheng, C. C., Lai, C. C., Hsu, J. L., Chang, W. J., Chiang, S. Y., Lee, H. J., Liao, H. W., Chuang, P. H., Chen, H. Y., Wang, H. L., Kuo, S. C., Chen, C. H., Yu, Y. L., and Hung, M. C. (2014) EGFR modulates DNA synthesis and repair through Tyr phosphorylation of histone H4. *Dev. Cell* **30**, 224-237

Acknowledgments- We are grateful to Dr. Donald J. Fujita (University of Calgary), Dr. Tadashi Yamamoto (The University of Tokyo), Dr. Eli Canaani (Weizmann Institute of Science), Dr. Toshiki Tamura (National Institute of Infectious Diseases), Dr. Takayuki Yoshimoto (Tokyo Medical University), Dr. Edward A. Clark (University of Washington), Dr. Shigeyuki Yokoyama (RIKEN), Dr. Hiroyuki Miyoshi (RIKEN BRC), for their invaluable plasmids and antibodies. We are also grateful to Mr. Takahiko Murayama for his technical assistance. This work was supported in part by grants-in-aid for Scientific Research C (N.Y., 25460356) and JSPS fellows (S.K., 264367), Global COE Program (G-COE, Global Center for Education and Research in Immune Regulation and Treatment), and Program for Leading Graduate Schools (LGS, Nurture of Creative Research Leaders in Immune System Regulation and Innovative Therapeutics) from the Japanese Ministry of Education, Culture, Sports, Science and Technology. K.A. and S.K. were G-COE Research Assistants. S.K. is a Research Fellow of Japan Society for the Promotion of Science. M.M. is a LGS Research Assistant.